Dual-Lanthanide-Chelated Silica Nanoparticles as Labels for Highly Sensitive Time-Resolved Fluorometry

Heng Zhang,[†] Ye Xu,[†] Wei Yang,[†] and Qingge Li*[,†,‡]

Molecular Diagnostics Laboratory, Department of Biomedical Sciences and the Key Laboratory of the Ministry of Education for Cell Biology and Tumor Cell Engineering, School of Life Sciences, Xiamen University, Xiamen, Fujian 361005, China, and The Key Laboratory of Chemical Biology of Fujian, Xiamen University, Xiamen, Fujian 361005, China

Received April 1, 2007. Revised Manuscript Received September 7, 2007

We have synthesized dual-lanthanide-chelated silica nanoparticles for potential use as labels in bioanalysis. A universal ligand 2,9-bis[*N*,*N*-bis(carboxymethyl)aminomethyl]-1,10-phenanthroline that could bind both Eu(III) and Tb(III) was covalently linked with 3-aminopropyl(triethoxy) silane to form silica nanoparticles in the presence of precisely controlled ratios of Eu(III)/Tb(III). The nanoparticles thus prepared could have specified ratios of luminescence intensities at two well-resolved emissions under a single-wavelength excitation. After comprehensive characterization with respect to their fluorescence lifetime, photostability, thermostability, and chelate leakage, a practical use of these nanoparticles was evaluated in a time-resolved immunofluorometric assay of human hepatitis B surface antigen. The results showed much increased sensitivity and quantification ranges than the enzyme-linked immunosorbent assay, demonstrating the suitability and advantages of these nanoparticles for bioassays.

Introduction

The development of multiplexed and highly sensitive bioassays is becoming increasingly important for simultaneous detection of biomarkers present at low concentration. Multiplexed assays reduce the time and cost per analysis, allow for simplified assay protocols, decrease the sample volumes required, and most importantly, make measurement of the closely related disease markers in a sample feasible, reproducible, and reliable. On the other hand, a highly sensitive assay system is needed to detect disease markers at their emerging stage for early diagnosis. Conventional fluorophore-labeled assay systems can handle a high degree of multiplexed detection using spatially resolved measurements; however, they lack the sensitivity requested for many disease markers and the experimental equipments are not convenient to use on a routine basis. A variety of microspheres and nanoparticles, such as quantum dots (QDs),[1–4] gold nanoparticles,[5–7] dye-doped silica nanoparticles,[8–10] and fluorescent polystyrene particles,[11,12] have been explored to be alternatives, with their unique advantages of strong signal and potential for wavelength and intensity multiplexing. However, it is not easy to carry out parallel coding on the nanometer scale, and because of the difficulty in the separation of the target and background signals, the expected high sensitivity remains to be achieved.

Fluorescent lanthanide chelates are very noticeable as fluorescence probes for a highly sensitive time-resolved immunofluorometric assay (TrIFA), a DNA hybridization assay, and fluorescence imaging microscopy.[13–17] Their long lifetimes allow for better separation between signal and noise when detected in time-resolved mode. In addition, the large Stokes shift and sharp emission spectra further eliminate the background interference. Because different lanthanides have their unique fluorescence emission, multiplex assays using different lanthanide chelate labels have been developed.[18–20] However, the fluorescence of lanthanide chelates is generally weaker than organic fluorescent dyes, preventing their direct applications in multiplexed and highly sensitive bioassays.

* To whom correspondence should be addressed. Telephone: 86-0592-2182100. Fax: 86-0592-2187363. E-mail: qgli@xmu.edu.cn.
[†] School of Life Sciences, Xiamen University.
[‡] The Key Laboratory of Chemical Biology of Fujian, Xiamen University.

(1) Gao, X.; Yang, L.; Petros, J. A.; Marshall, F. F.; Simons, J. W.; Nie, S. *Curr. Opin. Biotechnol.* **2005**, *16*, 63.
(2) Chan, W. C.; Nie, S. *Science* **1998**, *281*, 2016.
(3) Taylor, J. R.; Fang, M. M.; Nie, S. *Anal. Chem.* **2000**, *72*, 1979.
(4) Gao, X.; Cui, Y.; Levenson, R. M.; Chung, L. W.; Nie, S. *Nat. Biotechnol.* **2004**, *22*, 969.
(5) Taton, T. A.; Mirkin, C. A.; Letsinger, R. L. *Science* **2000**, *289*, 1757.
(6) Lytton-Jean, A. K.; Mirkin, C. A. *J. Am. Chem. Soc.* **2005**, *127*, 12754.
(7) Li, H.; Rothberg, L. J. *Anal. Chem.* **2004**, *76*, 5414.
(8) Santra, S.; Zhang, P.; Wang, K.; Tapec, R.; Tan, W. *Anal. Chem.* **2001**, *73*, 4988.
(9) Santra, S.; Wang, K.; Tapec, R.; Tan, W. *J. Biomed. Opt.* **2001**, *6*, 160.
(10) Lian, W.; Litherland, S. A.; Badrane, H.; Tan, W.; Wu, D.; Baker, H. V.; Gulig, P. A.; Lim, D. V.; Jin, S. *Anal. Biochem.* **2004**, *334*, 135.
(11) Ji, J.; Rosenzweig, N.; Griffin, C.; Rosenzweig, Z. *Anal. Chem.* **2000**, *72*, 3497.
(12) Seydack, M. *Biosens. Bioelectron.* **2005**, *20*, 2454.
(13) Diamandis, E. P.; Morton, R. C.; Reichstein, E.; Khosravi, M. J. *Anal. Chem.* **1989**, *61*, 48.
(14) Diamandis, E. P.; Christopoulos, T. K. *Anal. Chem.* **1990**, *62*, 1149A.
(15) Hemmila, I.; Dakubu, S.; Mukkala, V. M.; Siitari, H.; Lovgren, T. *Anal. Biochem.* **1984**, *137*, 335.
(16) Meurman, O. H.; Hemmila, I. A.; Lovgren, T. N.; Halonen, P. E. *J. Clin. Microbiol.* **1982**, *16*, 920.
(17) Siitari, H.; Hemmila, I.; Soini, E.; Lovgren, T.; Koistinen, V. *Nature* **1983**, *301*, 258.
(18) Barnard, G.; Kohen, F. *Clin. Chem.* **1998**, *44*, 1520.
(19) Xu, Y. Y.; Pettersson, K.; Blomberg, K.; Hemmila, I.; Mikola, H.; Lovgren, T. *Clin. Chem.* **1992**, *38*, 2038.
(20) Hemmila, I.; Holttinen, S.; Pettersson, K.; Lovgren, T. *Clin. Chem.* **1987**, *33*, 2281.

10.1021/cm070900f CCC: $37.00
Published on Web 10/23/2007

To increase the fluorescence intensity of lanthanide chelates, nanoparticles containing thousands of fluorescent lanthanide chelates have been developed for ultrasensitive TrIFA. Polystyrene nanoparticles doping with fluorescent Eu(III) chelates were first explored as ultrasensitive labels for detection of prostate-specific antigen.[21–25] Polystyrene nanoparticles doped with analogous fluorescent lanthanide chelates, e.g., Eu(III), Tb(III), Sm(III), and Dy(III) chelates, were also reported as potential multiplexing labels.[22] However, current polystyrene nanoparticles suffer from drawbacks, such as the risk of chelate leaking from the nanoparticles, the tendency to agglomerate in aqueous medium, and difficulties in separation from the solution. Recently, silica nanoparticles with their inherent hydrophilicity, flexible surface modification, and ready separation from solution have become alternative scaffolds for lanthanide-chelating loading.[26–29] Attractively, these silica nanoparticles could be prepared by covalently linking lanthanide chelates to the silica nanoparticles, and thus, the leaking problem is well-solved.[30–34] However, functional lanthanide chelates are of limited availability. Thus far, only Eu(III) chelates have been covalently linked with silica nanoparticles and have been evaluated as labels for TrIFA,[26,27] whereas a multiplexed assay using lanthanide chelate-containing silica nanoparticles has never been explored.

We report here the preparation of a unique chelator that could bind to both Eu(III) and Tb(III) and give their typical fluorescence. This chelator was covalently linked to a silane, which could be co-polymerized with tetraethyloxyl orthosilicate (TEOS) to form silica nanoparticles. Single-wavelength excitation with dual emission endows the nanoparticles with optical encoding capability for multiplexed detection. The covalently linked fluorescence silica nanoparticles were evaluated in parallel with polystyrene nanoparticles in photostability and thermostability. Finally, as a model of application, the TrIFA of human hepatitis B surface antigen (HBsAg) was developed using the Tb(III)-incorporated silica nanoparticles.

Experimental Section

Materials. 2,9-Bis[*N*,*N*-bis(carboxymethyl)aminomethyl]-1,10-phenanthroline (BBCAP) was synthesized as described previously.[35] OptiLink carboxylate-modified polystyrene microparticles (CM-MPs) were purchased from Seradyn, Inc. and were separated from solution by a Nanosep ultracentrifuge filter (10 kDa cutoff; Pall filter). Horseradish peroxidase (HRP)-labeled anti-HBsAg monoclonal antibody and goat polyclonal and mouse monoclonal anti-HBsAg antibodies were provided by InTec Products, Inc. White opaque microtitration plates (Costar 3922) were purchased from Corning, Inc. The standard solutions of HBsAg were prepared by diluting HBsAg (InTec Products, Inc.) with 0.05 M Tris-HCl buffer containing 5% bovine serum albumin (BSA), 0.9% NaCl, and 0.1% NaN_3 (pH 7.8). Unless otherwise stated, all chemical materials were purchased from commercial sources and used without further purification. Ultrapure water (18.0 MΩ) was used throughout the experiments.

Instrumentation. Mass spectra were recorded on a Bruker Dalton Esquire 3000 plus electrospray ionization mass spectrometry (ESI/MS). ^{1}H nuclear magnetic resonance (NMR) spectra were recorded on a Varian Unity plus 500 M NMR spectrometer. Infrared absorption spectra were measured on an Avatar 360 Fourier transform infrared (FTIR) spectrometer. Luminescence spectra and lifetimes were measured on a Varian Cary Eclipse fluorescence spectrophotometer. UV–vis absorption spectra were measured on a Beijing Purkinje General TU-1900 spectrometer. The shape and size of nanoparticles were characterized using a JEOL JEM-2100 (100 kV) transmission electron microscope. Photobleaching experiments were carried out on a Hitachi F-4010 fluorescence spectrophotometer. Element analysis of lanthanide was performed using a HP 4500 inductively coupled plasma mass spectrometry (ICP–MS). The TrIFA of HBsAg using Tb(III)-incorporated silica nanoparticles was carried out on microtitration plates and measured on a Perkin-Elmer Victor^2 1420 multilabel counter with the following conditions: excitation wavelength of 320 nm, emission wavelength of 545 nm, delay time of 0.5 ms, and window time of 1.4 ms. An enzyme-linked immunosorbnent assay (ELISA) for HBsAg was carried out on a Molecular Device Corp. SpectraMax M2 microplate reader.

Preparation of Dual-Lanthanide-Chelated Silica Nanoparticles. The functionalized precursor APS-BBCAP-Eu(III)/Tb(III) conjugate was prepared as follows. BBCAP (2.0 mg in 20 μL of sodium carbonate buffer, 0.05 M, pH 9.5) was added to a mixture containing 6.4 mg of 1-ethyl-3-(3-dimethylaminopropyl)carbodiimide hydrochloride (EDC) and 2.0 mg of *N*-hydroxysulfosuccinimide (NHS) in 80 μL of anhydrous ethanol. The mixture was agitated for 20 min, followed by the addition of 1.5 μL of (3-aminopropyl)trimethoxylsilane (APTMS). The reaction was allowed to continue for another 2 h. Then, a mixed solution of $EuCl_3$ and $TbCl_3$ (200 μL, 0.01 M) with a molar ratio of 0:1, 1:3, 1:1, 3:1, and 1:0 was added. For nanoparticles preparation, Triton X-100, 1-hexanol, and cyclohexane (1:1:3, v/v) were added to a flask while stirring to make a homogenous solution. To 10 mL of this solution, 100 μL of the functionalized precursor and 300 μL of water were added while stirring to obtain a W/O microemulsion. After the addition of 100 μL of TEOS with vigorous stirring, the polymerization reaction was initiated by adding 60 μL of concentrated NH_4OH (25–28%). The reaction was allowed to continue for 24 h at room temperature. The final silica nanoparticles were washed continuously with acetone, ethanol, and water several times to remove the surfactant and unreacted materials.

(21) Harma, H.; Soukka, T.; Lovgren, T. *Clin. Chem.* **2001**, *47*, 561.
(22) Huhtinen, P.; Kivela, M.; Kuronen, O.; Hagren, V.; Takalo, H.; Tenhu, H.; Lovgren, T.; Harma, H. *Anal. Chem.* **2005**, *77*, 2643.
(23) Valanne, A.; Huopalahti, S.; Vainionpaa, R.; Lovgren, T.; Harma, H. *J. Virol. Methods* **2005**, *129*, 83.
(24) Vaisanen, V.; Harma, H.; Lilja, H.; Bjartell, A. *Luminescence* **2000**, *15*, 389.
(25) Soukka, T.; Paukkunen, J.; Harma, H.; Lonnberg, S.; Lindroos, H.; Lovgren, T. *Clin. Chem.* **2001**, *47*, 1269.
(26) Hai, X.; Tan, M.; Wang, G.; Ye, Z.; Yuan, J.; Matsumoto, K. *Anal. Sci.* **2004**, *20*, 245.
(27) Tan, M.; Wang, G; Hai, X; Ye, Z; Yuan, J. *J. Mater. Chem.* **2004**, *14*, 2896.
(28) Tan, M.; Ye, Z.; Wang, G.; Yuan, J. *Chem. Mater.* **2004**, *16*, 2494.
(29) Ye, Z.; Tan, M.; Wang, G.; Yuan, J. *Anal. Chem.* **2004**, *76*, 513.
(30) Soares-Santos, P. C. R.; Nogueira, H. I. S.; Felix, V.; Drew, M. G. B.; Ferreira, R. A. S.; Carlos, L. D.; Trindade, T. *Chem. Mater.* **2003**, *15*, 100.
(31) Binnemans, K.; Lenaerts, P.; Driesen, K.; Gorller-Walrand, C. *J. Mater. Chem.* **2004**, *14*, 191.
(32) Lenaerts, P.; Driesen, K.; van Deun, R.; Binnemans, K. *Chem. Mater.* **2005**, *17*, 2148.
(33) Lenaerts, P.; Storms, A.; Mullens, J.; D'Haen, J.; Gorller-Walrand, C.; Binnemans, K.; Driesen, K. *Chem. Mater.* **2005**, *17*, 5194.
(34) Sun, L.-N.; Zhang, H.-J.; Peng, C.-Y.; Yu, J.-B.; Meng, Q.-G.; Fu, L.-S.; Liu, F.-Y.; Guo, X.-M. *J. Phys. Chem. B* **2006**, *110*, 7249.
(35) Lin, P.; Zheng, H.; Zhu, Q.; Xu, J. *Microchim. Acta* **2002**, *140*, 125.

Preparation of Nanoparticle-Labeled Antibody. First, amino groups were introduced to the nanoparticle surfaces as follows. Silica nanoparticles (10 mg) were suspended in 1.0 mL of anhydrous ethanol, to which 1.5 μL of APTMS was added under stirring. After agitation for 2 h at room temperature, the nanoparticles were centrifuged and washed with ethanol 3 times and stored in anhydrous ethanol. Before labeling, the antibody was first oxidized to produce aldehyde groups. To do so, 200 μL of 2 mg/mL anti-HBsAg IgG solution was dialyzed against acetate buffer (0.01 M, pH 5.2) at 4 °C, followed by the addition of 10 μL of 0.5 M $NaIO_4$. After gentle stirring for 20 min in the darkness at room temperature, the reaction was terminated by adding 2 μL of glycerol under continuous stirring for 10 min. The solution was then dialyzed against the acetate buffer at 4 °C overnight to remove residual small molecules. To label the antibody with nanoparticles, the dialyzed antibody solution was adjusted to pH 9.0 with 0.1 M Na_2CO_3, followed by the addition of 4 mg of aminated nanoparticles suspended in carbonate buffer (0.01 M, pH 9.0). After stirring for 12 h at 4 °C, $NaBH_4$ was added to the final concentration of 5 mM and the reaction was allowed to continue for 12 h at 4 °C. The reaction was terminated by adding an equal volume of blocking buffer (0.01 M Tris-HCl containing 2% BSA, 4% sucrose, and 1% glycine at pH 7.8). After incubation for 12 h at 4 °C, these nanoparticles were rinsed with 0.01 M Tris-HCl (pH 7.8) 3 times. Finally, the antibody-linked nanoparticles were collected and resuspended in 400 μL of dilution buffer (0.01 M Tris-HCl containing 0.9% NaCl, 0.2% BSA, and 0.1% NaN_3 at pH 7.8) and stored at 4 °C before use.

Immunoassays. The TrIFA of HBsAg using Tb(III)-incorporated silica nanoparticles were performed as follows: Anti-HBsAg monoclonal antibody (diluted to 5 μg/mL in 0.02 M Tris-HCl buffer at pH 7.4) was first physically coated on the microplate wells (50 μL per well), and then 50 μL of HBsAg standard solution was added to each well. The plate was incubated at 37 °C for 45 min and washed 3 times with washing buffer 1 (0.01 M PBS buffer and 0.05% Tween 20 at pH 7.4). Then, 50 μL of antibody-linked Tb(III)-incorporated silica nanoparticles (diluted 500-fold with the dilution buffer) was added to each well. The plate was incubated at 37 °C for 90 min and washed 5 times with washing buffer 2 (0.01 M Tris-HCl buffer and 0.05% Tween 20 at pH 9.1). Finally, the plate was subjected to solid-phase time-resolved fluorometric measurement.

Standard ELISA was carried out as follows: Anti-HBsAg monoclonal antibody (diluted to 5 μg/mL with 0.02 M Tris-HCl buffer at pH 7.4) was coated on microplate wells (50 μL per well), following by the addition of 50 μL of HBsAg standard solution and 50 μL of HRP-labeled anti-HBsAg monoclonal antibody and incubated for 2 h at 37 °C. The wells were washed 3 times with washing buffer 1, and color development was produced using H_2O_2 and tetramethylbenzidine (TMB). The reaction was stopped with 2 M H_2SO_4, and absorbance was determined at 450 nm by a microplate reader.

Results

Preparation and Characterization of Lanthanide-Chelated Nanoparticles. BBCAP synthesized was identified by means of ESI/MS, IR, HNMR, and UV–vis. The molecular weight measured by ESI/MS was 471.30, which is analogous with its theoretical mass value of 470.43. UV–vis absorption characteristic peaks: 231 and 272 nm. IR absorption characteristic peaks (KBr): 3435, 3008, 1704, 1628, 1405, and 1229 cm^{-1}. ^1H NMR (500 MHz, D_2O): 3.287 (s, 8H), 4.107 (s, 4H), 7.556 (s, 2H), 7.640 (d, J = 8.0, 2H), 8.134 (d, J = 7.5, 2H).[35] The luminescence spectrum of BBCAP–Eu(III) had four lines, i.e., 592 nm ($^5D_0 \rightarrow {}^7F_1$), 615 nm ($^5D_0 \rightarrow {}^7F_2$), 653 nm ($^5D_0 \rightarrow {}^7F_3$), and 694 nm ($^5D_0 \rightarrow {}^7F_4$), respectively, and the maximum fluorescence intensity was at 615 nm. The luminescence spectrum of BBCAP–Tb(III) had four lines, i.e., 490 nm ($^5D_4 \rightarrow {}^7F_6$), 545 nm ($^5D_4 \rightarrow {}^7F_5$), 583 nm ($^5D_4 \rightarrow {}^7F_4$), and 621 nm ($^5D_4 \rightarrow {}^7F_3$), and the maximum fluorescence intensity was at 545 nm. The intensity ratio I ($^5D_0 \rightarrow {}^7F_2$)/($^5D_0 \rightarrow {}^7F_1$) in the europium spectra was ca. 3.0 using the integrated intensity values.

Silica nanoparticles were prepared by co-hydrolysis of TEOS with the lanthanide chelate functionalized precursor catalyzed by ammonium hydroxide in a W/O microemulsion (Figure 1). Silica nanoparticles prepared were spherical and uniform in size (40 ± 5 nm in diameter). A closer look showed that, unlike physical doping, no black spots were found inside these nanoparticles.[29] Thus, we concluded that covalently linked lanthanide chelate distributed evenly throughout the silica network rather than form clusters (Figure 2). A fluorometric measurement showed that the ability of BBCAP to chelate both Eu(III) and Tb(III) was well kept in the form of nanoparticles, and identical lanthanide fluorescence excitation and emission spectra were observed with free chelates (parts A and B of Figure 3). A time-resolved measurement showed that, in aqueous solution, the fluorescence lifetime of both Eu(III)- and Tb(III)-incorporated silica nanoparticles had a longer fluorescence lifetime than their corresponding free chelates. For Eu(III)-incorporated silica nanoparticles, the lifetime was 1.20 ms, while the lifetime for free BBCAP–Eu(III) was 0.42 ms. For Tb(III)-incorporated silica nanoparticles, the lifetime was 1.95 ms, while the lifetime for free BBCAP–Tb(III) chelate in aqueous solution was 0.64 ms. These results indicated that the lanthanide chelates were better protected from fluorescence quenching than the free chelate in aqueous solution.

Because BBCAP could bind both Eu(III) and Tb(III), different fluorescence emission spectra could be obtained when excited at the same wavelength. If only Eu(III) was chelated, typical Eu fluorescence was observed. If only Tb(III) was chelated, typical Tb fluorescence was observed. If both Eu(III) and Tb(III) were chelated, both of their fluorescence was observed and their hybrid fluorescence spectrum changed with a different ratio of Eu(III)/Tb(III) (Figure 3C). Thus, by adjusting the relative amount of Eu(III) and Tb(III), a variety of emission spectra could be obtained. As shown in Figure 3D, these nanoparticles could display different fluorescent colors under a single UV light source. Eu(III)-incorporated silica nanoparticles displayed a red color; Tb(III)-incorporated silica nanoparticles displayed a green color; and the hybrid Eu(III)/Tb(III)-incorporated silica nanoparticles displayed mixed red and green colors.

Photostability and Thermostability. The less fluorescence quenching found in the lanthanide chelates encapsulated in silica nanoparticles implied better photostability than free chelates. To validate this hypothesis, both Eu(III)-incorporated silica nanoparticles and free BBCAP–Eu(III) chelate solution were exposed to continuous UV illumination in a fluorometer with Hg lamp as the light source and the fluorescence intensity was measured continuously. The

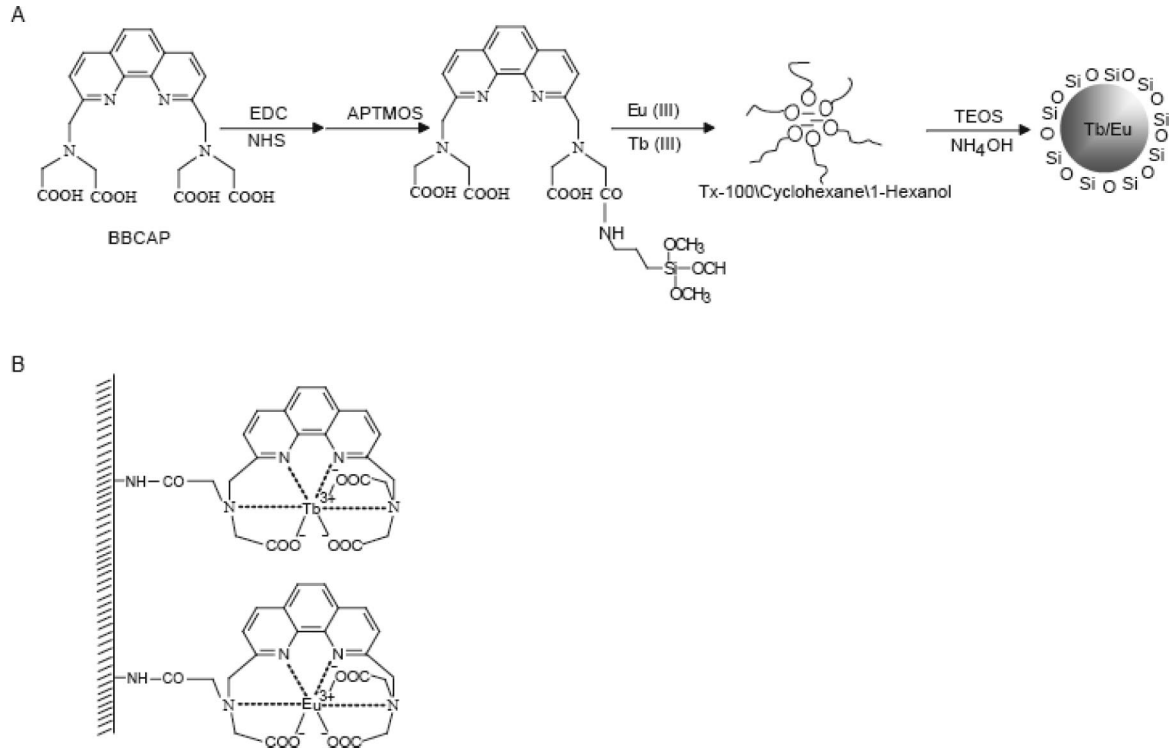

Figure 1. Schematic representation of the preparation process of dual-lanthanide-chelated silica nanoparticles (A) and the Eu(III)/Tb(III) chelates (B) covalently encapsulated in the silica network (shadow).

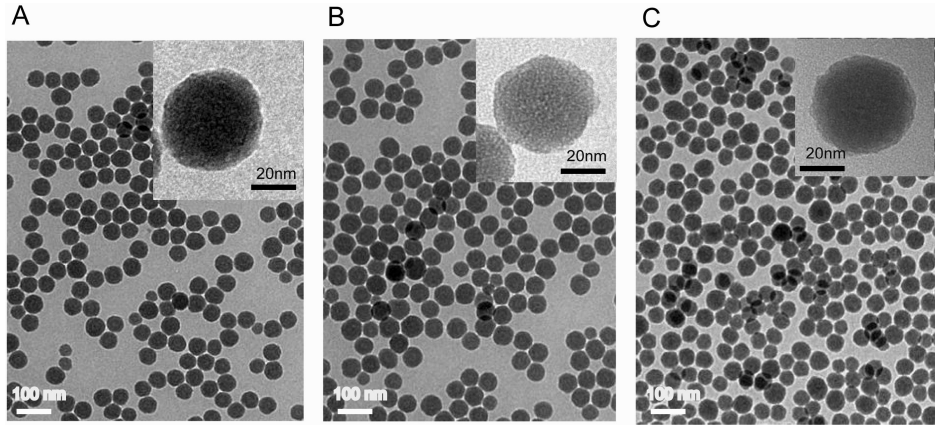

Figure 2. Transmission electron microscopy (TEM) images of Tb(III) silica nanoparticles (A), Eu(III) silica nanoparticles (B), and Eu(III)/Tb(III) silica nanoparticles (C). The insets show higher resolution images of the same nanoparticles.

commercial latex nanoparticles, CM-MPs, which contain fluorescent Eu–thienyltrifluroacetone (TTA) chelates were also studied in parallel as a comparison. The results showed that the Eu(III)-incorporated silica nanoparticles did not show an obvious fluorescence decrease, whereas the fluorescence of free chelate BBCAP–Eu(III) gradually declined (Figure 4). Surprisingly, CM-MPs were even less stable than free BBCAP, and their fluorescence rapidly went down. These results demonstrated that the lanthanide chelates encapsulated inside the silica nanoparticles were better protected from photobleaching than free chelates in solution and those doped in polystyrene particles. The photostability of lanthanide encapsulated inside silica nanoparticles agreed with previous reports.[36–39]

We then compared the thermostability of both Eu(III)-incorporated silica nanoparticles and CM-MPs stored in different buffer at 4 and 37 °C, respectively. As shown in Figure 5, although there was an intensity difference among different buffer, both Eu(III)-incorporated silica nanoparticles and CM-MPs were stable at 4 °C regardless of the buffer type. It was noted however, in ethanol, that the fluorescence of CM-MPs was strongly quenched, while Eu(III)-incorporated silica nanoparticles showed only a slight decrease. When placed at 37 °C, Eu(III)-incorporated silica nanoparticles were still stable in both 0.01 M Tris-HCl at pH 7.8 (Tris buffer) and ethanol but became unstable in 0.01 M Tris-

(36) Lima, P. P.; Ferreira, R. A. S.; Freire, R. O.; Paz, F. A. A.; Fu, L. S.; Alves, S.; Carlos, L. D.; Malta, O. L. *ChemPhysChem* **2006**, *7*, 735.
(37) Nockemann, P.; Beurer, E.; Driesen, K.; van Deun, R.; van Hecke, K.; van Meervelt, L.; Binnemans, K. *Chem. Commun.* **2005**, *34*, 4354.
(38) Qian, G. D.; Wang, M. Q. *J. Am. Ceram. Soc.* **2000**, *83*, 703.
(39) Gameiro, C. G.; Achete, C. A.; Simao, R. A.; da Silva, E. F.; Santa-Cruz, P. A. *J. Alloys Compd.* **2002**, *344*, 385.

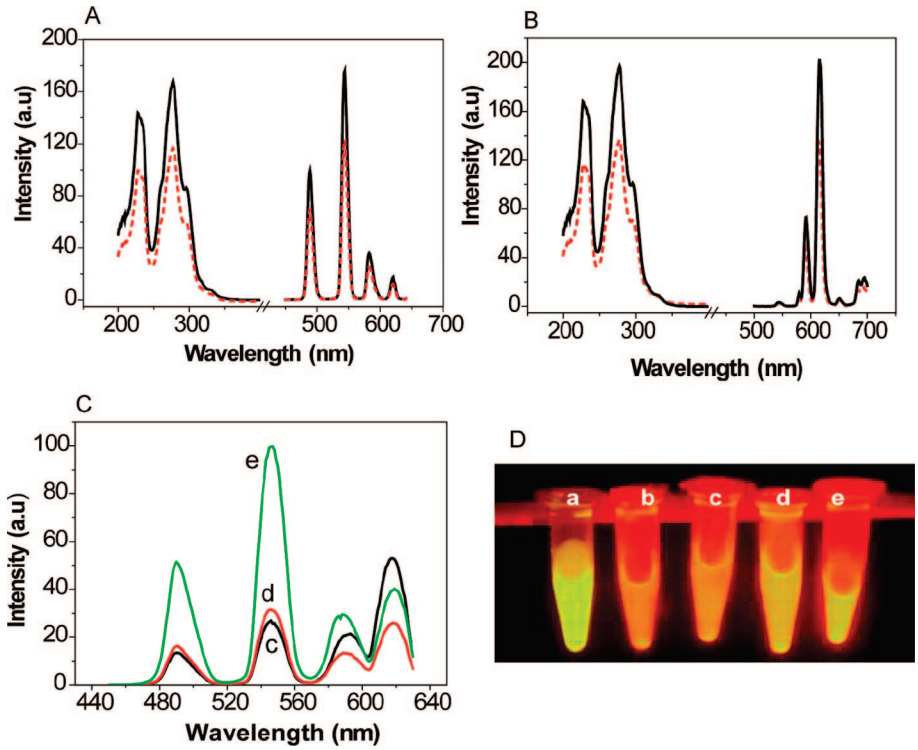

Figure 3. Spectrum characteristics of Eu(III)-, Tb(III)-, and Eu(III)/Tb(III)-incorporated silica nanoparticles. The following conditions were used for spectra measurements: delay time of 0.2 ms, gate time of 0.4 ms, cycle time of 20 ms, excitation slit of 5 nm, and emission slit of 5 nm. (A) Excitation and emission spectra of Tb(III)-incorporated silica nanoparticles (—) and pure BBCAP–Tb(III) (- - -). Excitation spectra were recorded with $\lambda_{em} = 545$ nm, and emission spectra were recorded with $\lambda_{ex} = 280$ nm. (B) Excitation and emission spectra of Eu(III)-incorporated silica nanoparticles (—) and pure BBCAP–Eu(III) chelate (- - -). Excitation spectra were recorded with $\lambda_{em} = 615$ nm, and emission spectra were recorded with $\lambda_{ex} = 280$ nm. (C) Emission spectra of Eu(III)/Tb(III)-incorporated silica nanoparticles according to the different ratios of Tb(III)/Eu(III) in sodium carbonate buffer were measured by time-resolved luminescence mode under the above conditions. (D) Photograph of Eu(III)/Tb(III) silica nanoparticles in dilute ethanol solution under irradiation of a 254 nm Hg lamp: a, Tb(III) silica nanoparticles; b, Eu(III) silica nanoparticles; c, Eu(III)/Tb(III) = 3:1; d, Eu(III)/Tb(III) = 1:1; e, Eu(III)/Tb(III) = 1:3.

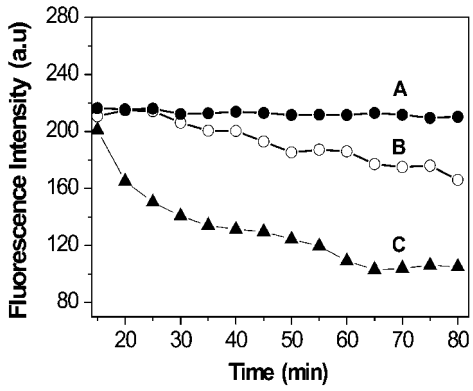

Figure 4. Comparison of the photostability of Eu(III)-incorporated silica nanoparticles (A), BBCAP–Eu(III) chelate (B), and CM-MPs (C) in aqueous solution phase under continuous UV irradiation.

HCl at pH 7.8 containing 0.05% Tween 20 (Trist buffer). In contrast, the fluorescence of CM-MPs rapidly decreased in both Tris and Trist buffer and completely disappeared in ethanol. Collectively, these results demonstrated that Eu(III)-incorporated silica nanoparticles were more thermostable than CM-MPs in different solutions at different temperatures.

One possible reason for the above phenomena could be ascribed to the varied leakage degree of lanthanide chelates from the particles. To verify this assumption, we used ICP–MS to determine the amount of lanthanide leaking out of the nanoparticles. Eu(III)-incorporated silica nanoparticles were washed with water 3 times, and the supernatant of the last washing was collected and used as the control. The nanoparticles were then suspended in 70% ethanol and Trist buffer, respectively, and stored at 4 °C for 1 week. The nanoparticles were centrifuged, and the supernatant was collected. The washing solution together with the nanoparticles suspension and the supernatant were all diluted 3 times and subjected to ICP–MS analysis. For a comparison, CM-MPs were also treated and analyzed in the same way. Unlike Eu(III)-incorporated silica nanoparticles, CM-MPs were rather difficult to be separated from the solution by centrifugation because of its low density; they were however washed and separated using a Nanosep ultracentrifuge filter. As shown in Figure 6, the leakage of Eu(III) was much less in silica nanoparticles than in CM-MPs. The leakage degree of both particles was greater when stored in ethanol than in Trist buffer.

Time-Resolved Immunofluorometric Assay of Human HBsAg. We evaluated the lanthanide-incorporated silica nanoparticles as labels for TrIFA. A typical sandwich TrIFA for HBsAg was developed on the basis of Tb(III)-incorporated silica nanoparticles. The detection antibody was labeled with the Tb(III)-incorporated silica nanoparticles using a site-specific labeling strategy that allows for the binding sites of the labeled antibody to orient away from the nanoparticles and toward the antigen. The calibration curves of HBsAg

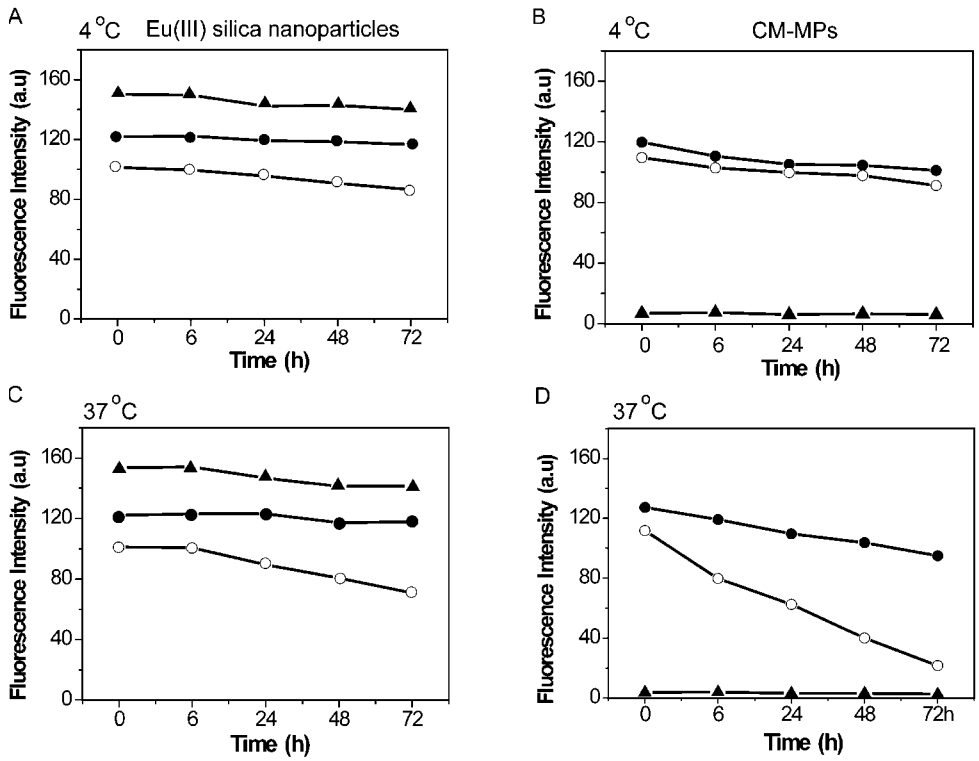

Figure 5. Comparison of the thermostability between Eu(III)-incorporated silica nanoparticles and CM-MPs. Eu(III)-incorporated silica nanoparticles (A and C) and CM-MPs (B and D) were studied in parallel at 4 and 37 °C, respectively, in three different solutions: Tris buffer (●), Trist buffer (○), and ethanol (▲).

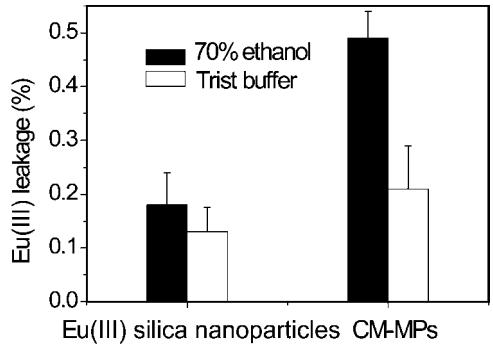

Figure 6. ICP–MS analysis of Eu(III) leakage from Eu(III)-incorporated silica nanoparticles and CM-MPs latex.

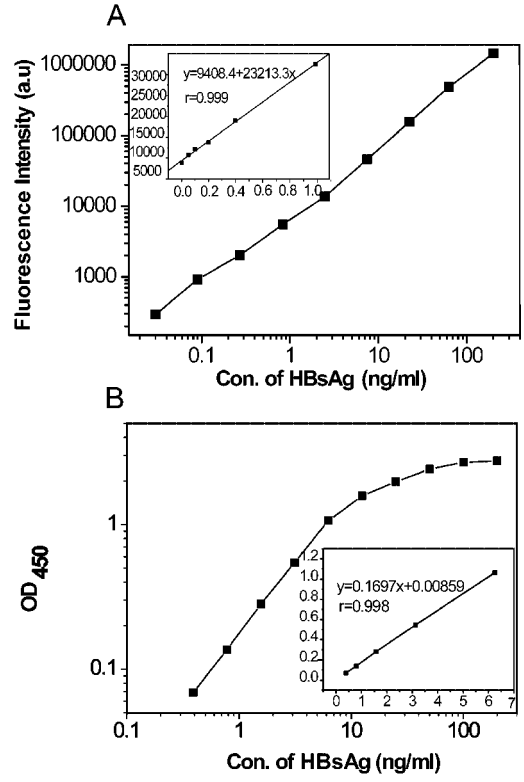

Figure 7. Calibration curves for HBsAg using Tb(III)-incorporated silica nanoparticles-based TrIFA (A) and ELISA (B). The inset curves show the low concentration part of the calibration curves.

are shown in Figure 7A. The detection limit, calculated with the concentration corresponding to 3 times the standard deviations of the background signal, was 35 pg/mL. The upper limit of the calibration curve was ca. 200 ng/mL. The coefficients of variation (CVs) across the whole range are below 8.9%. In comparison, under the same conditions, the detection limit of ELISA was 200 pg/mL and the upper limit of the calibration curve was ca. 10 ng/mL (Figure 7B).

Discussion

We described the covalent linkage of a lanthanide ligand capable of binding both Tb(III) and Eu(III) within silica nanoparticles. When the molar ratio of Eu(III)/Tb(III) was changed, nanoparticles could be prepared with different fluorescent emission spectra but with the same excitation spectrum. These nanoparticles could display multiple emission patterns under a single light source. To our knowledge, this is the first paper describing the preparation of such dual lanthanide-chelated nanoparticles. Because Eu(III) and Tb(II) chelates possess the highest fluorescence efficiency among

all of the luminescent lanthanide chelates, multiplex detection could be expected using these nanoparticles.

A variety of dual chelate-incorporated silica nanoparticles could be easily prepared by changing the relative ratio of Eu(III)/Tb(III) stoichiometrically. We had prepared a series of hybrid luminescent nanoparticles and observed the stoichiometric change of the emission spectra with different Eu(III)/Tb(III) ratios. Thus, we reasoned that there was negligible, if any, Tb^{3+}–Eu^{3+} energy transfer in the hybrid luminescent nanoparticles. The preparation for nanoparticles encapsulating fluorescent lanthanide chelates still faces many challenges. Physical doping is exclusively used in the latex nanoparticle and also often used in silica nanoparticle preparation. To decide whether certain lanthanide chelate could be doped or not, both physical and chemical compatibilities have to be considered. In the case of latex nanoparticles, emulsion is often the used method, which needs the chelates to be dissolved in a suitable organic reagent. The problem is that some fluorescent chelates may be hydrophilic and do not dissolve well in such an organic reagent.[40,41] Silica nanoparticles was much more flexible and compatible to both organic solvent and water solution; however, the chelates may not be encapsulated stably inside the silica network because of electrostatic repulsion.[42] In addition, physical doping inevitably leads to chelate leakage, impairing performance as a label in TrIFA.[28,29] Although the leakage problem has not been well-explored in the latex particle, its potential harm to the immunoassay has been noted.[43] As observed in this study, CM-MPs indeed have a leakage problem in the commonly used buffer. Chemical linkage could well address the leakage problem, but it needs functionalized groups in both the chelates and nanoparticles. Lanthanide ions often have their unique fluorogenic chelates, which are quite different with each other in chemical property. For example, many fluorogenic Eu(III) chelates are hydrophobic, whereas Tb(III) chelates are hydrophilic. Thus, varied conditions have to be tested to prepare suitable precursors, adding the overall difficulties in their preparations. In this context, a single chelator that could bind both Eu(III) and Tb(III) obviated all of these difficulties.

To be useful for a highly sensitive bioassay, the nanoparticle label should be stable enough under routine conditions. Our results demonstrated that the BBCAP-chelated nanoparticles were both photo- and thermostable compared to the latex nanoparticles under different conditions. Unlike latex nanoparticles, silica nanoparticles could be flexibly conjugated to different biomolecules and easily separated from the unlabeled biomolecules. As exemplified here, the surface of the Tb(III)-incorporated silica nanoparticles could be easily aminated and then conjugated to the antibody in a site-specific format. Because there are a variety of silanes possessing different functional groups, it is easy to find a suitable modification format for a target biomolecule. Moreover, the labeled antibody could be easily separated from the unlabeled antibody by a brief centrifugation. The TrIFA of HBsAg using Tb(III) silica nanoparticles showed a significantly increased quantification range compared to ELISA, demonstrating great potentials of these nanoparticles in highly sensitive TrIFA. It should be noted that the lanthanide-incorporated silica nanoparticles prepared here had short excitation wavelengths below 300 nm, which is unfavorable for their application as biolabels in time-resolved luminescence bioassays because of the lack of such a short excitation wavelength in the current instrument and potential hazard to the biological samples. However, for TrIFA, this disadvantage could be overcome simply by changing an appropriate excitation filter, so that even higher sensitivity could be achieved. Also, toxicity of lanthanide ions should be considered for in vivo assays. However, the toxicity is negligible when used in in vitro diagnosis, such as TrIFA.

Conclusions

A unique lanthanide chelate capable of binding both Eu(III) and Tb(III) was successfully covalently encapsulated into silica nanoparticles. The nanoparticles prepared could display typical fluorescence of Eu(III), Tb(III), or both simply by changing the ion ratio. Chimeric nanoparticles containing both Eu(III) and Tb(III) could be prepared that display a variety of fluorescent colors under a single light source. These nanoparticles have the advantages of uniform size distribution, strong fluorescence, great photostability and thermostability, long lifetime, leakage free, and flexible surface modification for site-specific bioconjugation. These properties altogether suggest their great potentials in sensitive and multiplexed bioassays.

Acknowledgment. We thank Dr. Peng Lin for help in BBCAP synthesis, Ms. Ping Chen for technical assistance in TEM imaging, and Zhixia Zhuang for ICP–MS analysis. This work was partially supported by the Fok Ying Tung Education Foundation, Education Ministry of China (104039).

CM070900F

(40) Hemmila, I.; Mukkala, V. M. *Crit. Rev. Clin. Lab. Sci.* **2001**, *38*, 441.
(41) Hemmila, I.; Laitala, V. *J. Fluoresc.* **2005**, *15*, 529.
(42) Bagwe, R. P.; Yang, C.; Hilliard, L. R.; Tan, W. *Langmuir* **2004**, *20*, 8336.
(43) Hakala, H.; Mukkala, V. M.; Sutela, T.; Hovinen, J. *Org. Biomol. Chem.* **2006**, *4*, 1383.